Geological Survey of Canada
Scientific Presentation 15

CLASSIFICATION OF WHOLE-ROCK GEOCHEMISTRY BASED ON STATISTICAL TREATMENT OF WHOLE-ROCK GEOCHEMICAL ANALYSES AND PORTABLE XRF ANALYSES AT THE ATTAWAPISKAT KIMBERLITE FIELD OF ONTARIO

E.C. Grunsky[1], B.A. Kjarsgaard[1], S. Kurszlaukis[2], M. Seller[2], R. Knight[1], and M. Moroz[1]

Whiskey Kimberlite

Introduction

A suite of whole-rock analyses of kimberlite from the Whiskey kimberlite in the Attawapiskat field, James Bay Lowlands (Figures 1 and 2), northern Ontario were provided to the Geological Survey of Canada, by De Beers Canada Exploration Ltd. for the purposes of undertaking statistical modeling to distinguish individual phases, and for examining the suitability of using a hand-held XRF spectrometer to distinguish these phases.

Methods Sampling and Analytical Methods

A database of 283 whole rock geochemical analyses were obtained from a selection of drill core samples. These samples were powdered and fused with lithium metaborate/tetraborate and then subsequently dissolved in a nitric acid digestion prior to major element analysis by ICP-ES and trace element analysis by ICP-MS or ICP-ES. All the provided raw geochemical data were subdivided into kimberlite type (e.g. U1VK, U2VK, U3VK) based on core logging and petrographic studies by De Beers geologists. The geochemical data utilized for the three phase kimberlite statistical model consisted of 189 whole-rock geochemical analyses (U1VK = 78; U2VK = 75, U3VK = 36). For analysed elements in the training data set in which the concentration was below detection (b.d.), the concentration was arbitrarily set to one-half of the detection limit.

Data Analysis and Statistical Methods

Major element oxide data was converted to cation% and then to ppm. Subsequently, the entire database was transformed by taking the log of the data normalized to bulk silicate Earth (pyrolite; McDonough and Sun, 1998). Based on an analysis of variance (Figure 3) for 44 analysed elements, a suite of 22 elements were selected for statistical treatment, with Al, Ta and Zr having the greatest discriminating power, and U, Ca and Na the least discriminating power. A principal component analysis (PCA) using the method outlined by Zhou et al., (1983) was applied to the log pyrolite-normalized data (for 22 elements). Ordered eigenvalues derived from the PCA are shown in Figure 4 as a screeplot of these ordered eigenvalues and their corresponding significance for the Whiskey dataset. The first three eigenvalues account for the majority (71%) of the variance of data. Figure 5 shows a plot of the kimberlite phases plotted on to the PC1-PC2 axes. The plot shows the relative relationships of the groups to the elements. Group U3VK has a relative increase in P, Mg, and Si, whereas group U2VK show a relative increase in Co, V, Ni, Fe, Ti, La, and Al. Group U1VK shows a relative increase in the abundances of Yb, Ta, Ga, Cr, and Ce. From the figure, it would appear that Group U3VK has a component of crustal contamination; group U2VK has a component of mantle material contamination, and group U1VK has a relative depletion of both mantle and crustal components.
Based on the selection of 22 elements, a linear discriminant analysis was carried out using a method of cross-validation to ensure robustness of the classification. Figure 6 shows a plot of the data plotted onto the first two linear discriminant axes. The group separation is good and the overall accuracy is 99.1%. Table 1 shows the classification accuracies for the three kimberlite phases. Based on the success of the classification using the whole rock geochemistry and a selected subset of elements, it was decided to investigate the evaluation of a portable hand-held XRF spectrometer as a tool for discriminating different kimberlite phases.

Preliminary analysis with Innov-X and Niton pXRF analyzer

Preliminary analysis, in 2008, was undertaken on both coarse crush and powders utilizing an Innov-X hand held analyzer at the GSC. Results via handheld spectrometry on coarse crush were unsatisfactory as compared to the whole rock geochemical data and this method of analysis was discontinued. The authors are of the opinion that this type of analysis will not provide meaningful results useful for exploration or mining applications. Analytical results on powders with the Innov-X pXRF were significantly better, however, the inability to analyze light elements (Si, Al, Mg, P) and high detection limits on other elements of interest as defined by analysis of variance on the Whiskey data set (Kjarsgaard and Grunsky, 2008) prompted tests with a newer model Niton XL3t GOLDD handheld XRF spectrometer (pXRF). The results from the coarse crush again proved unsatisfactory. The Niton instrument was calibrated for kimberlite analysis. Results of statistical treatment of the pXRF data, on powders, are shown in Figures 7, 8 and 9.

References

Grunsky, E.C. and Kjarsgaard, B.A., 2008. Classification of distinct eruptive phases of the diamondiferous Star Kimberlite, Saskatchewan, Canada based on statistical treatment of whole-rock geochemical analyses. Applied Geochemistry.

Kjarsgaard, B.A. and Grunsky,E.C. 2008. Analysis of Whole-rock powders from the Whiskey kimberlite, Attawapiskat Field, Ontario, Canada. Unpublished technical report to De Beers Canada.

McDonough, W.F., Sun, S.-S., 1995, The composition of the Earth: Chemical Geology, v.120 (3-4), p.223-253.

Zhou, D., Chang, T. and Davis, J.C., 1983: Dual extraction of R-Mode and Q-Mode factor solutions. Mathematical Geology 15 (5), p. 581-606.

Whiskey Kimberlite Geochemistry Multivariate Statistics

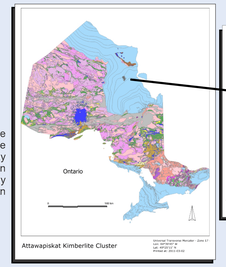

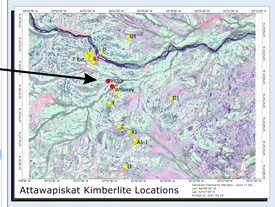

Figure 1. Location of the Attawpiskat kimberlite field, in the James Bay lowlands of northern Ontario. The Whiskey kimberlite is highlighted on the map.

Figure 2. Landsat ETM image of (bands 743) of the Attawapiskat kimberlite field south of the Attawapiskat River.

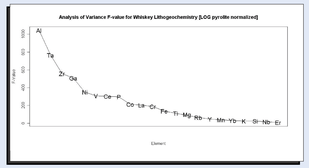

Figure 3. Analysis of variance F-values for 22 elements used to discriminate between the three kimberlite phases (U1VK, U2VK, U3VK), whole rock data.

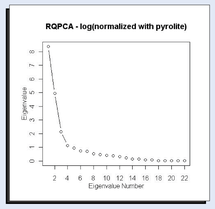

Figure 4. Screeplot of the eigenvalues obtained from a principal component analysis, whole rock data.

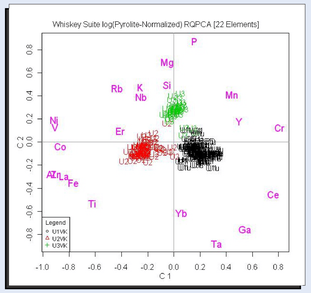

Figure 5. Biplot of the first two principal components of the Whiskey kimberlite phases based on 22 elements, whole rock data.

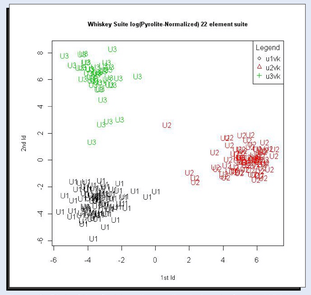

Figure 6. Plot of the first two linear discriminants for the Whiskey kimberlite data, whole rock data.

Table 1

Linear Discrminant Classification
Whiskey Kimberlite -pyrolite normalized

	Predicted		
	U1vk	U2vk	U3vk
U1vk	88	0	0
U2vk	0	86	0
U3vk	1	0	43

Percentage Classification	Predicted		
	U1vk	U2vk	U3vk
U1vk	100	0	0
U2vk	0	100	0
U3vk	2.73	0	97.73

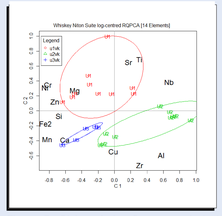

Figure 7. Biplot of the first two principal components of the Whiskey kimberlite phases based on 12 elements, calibrated Niton pXRF data.

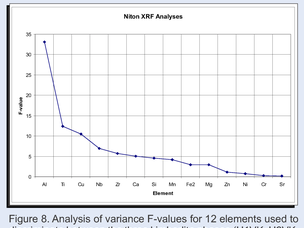

Figure 8. Analysis of variance F-values for 12 elements used to discriminate between the three kimberlite phases (U1VK, U2VK, U3VK), calibrated Niton pXRF data.

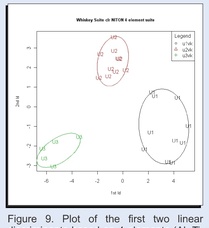

Figure 9. Plot of the first two linear discriminants based on 4 elements (Al, Ti, Cu and Nb) for the three kimberlite phases (U1VK, U2VK, U3VK), calibrated Niton pXRF data.

New pXRF Results - Niton Analyzer

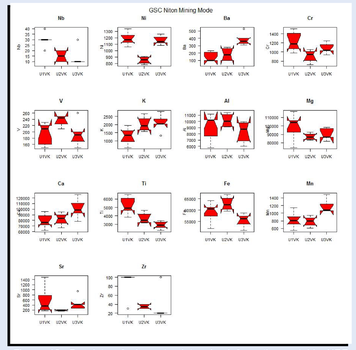

Figure 10. Boxplots of elements determined from the portable XRF analyzer in **Mining Mode** for the Whiskey kimberlite phases.

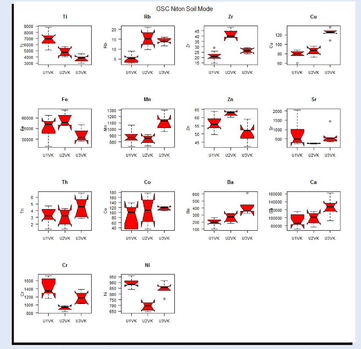

Figure 11. Boxplots of elements determined from the portable XRF analyzer in **Soil Mode** for the Whiskey kimberlite phases.

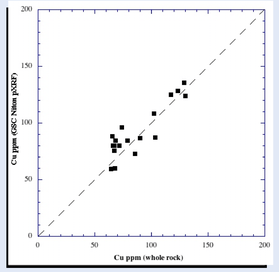

Figure 12. Plot of Cu determined by fusion/acid digestion and ICP analysis in the laboratory against Cu determined by portable XRF in **Mining Mode** for the Whiskey kimberlite phases.

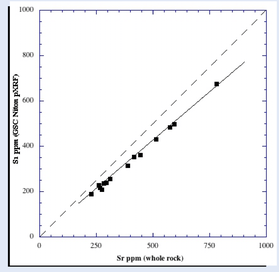

Figure 13. Plot of Sr determined by fusion/acid digestion and ICP analysis in the laboratory against Sr determined by portable XRF in **Mining Mode** for the Whiskey kimberlite phases.

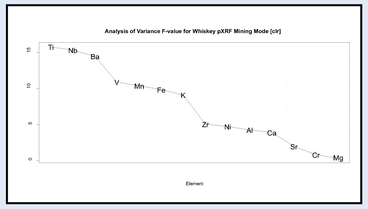

Figure 14. Analysis of variance F-values for 14 elements used to discriminate between the three kimberlite phases (U1VK, U2VK, U3VK) for the pXRF in **Mining Mode**.

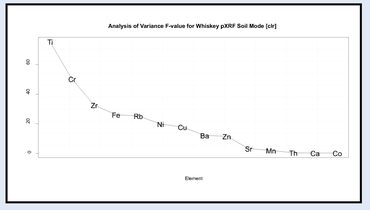

Figure 15. Analysis of variance F-values for 14 elements used to discriminate between the three kimberlite phases (U1VK, U2VK, U3VK) for the pXRF in **Soil Mode**.

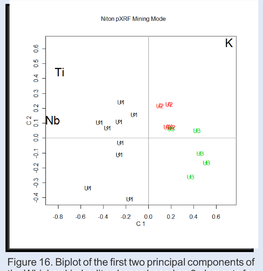

Figure 16. Biplot of the first two principal components of the Whiskey kimberlite phases based on 3 elements for the pXRF in **Mining Mode**.

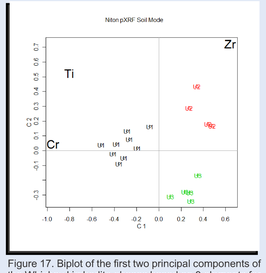

Figure 17. Biplot of the first two principal components of the Whiskey kimberlite phases based on 3 elements for the pXRF in **Soil Mode**.

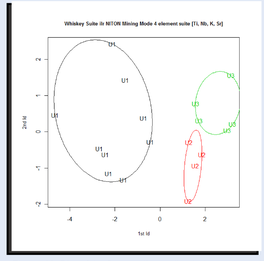

Figure 18. Plot of the first two linear discriminants based on 4 elements (Ti, Nb, K and Sr) for the three kimberlite phases (U1VK, U2VK, U3VK) for the pXRF in **Mining Mode**.

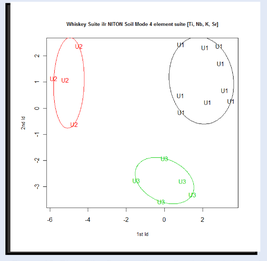

Figure 19. Plot of the first two linear discriminants based on 4 elements (Ti, Nb, K and Sr) for the three kimberlite phases (U1VK, U2VK, U3VK) for the pXRF used in **Soil Mode**.

New pXRF Results - Niton Analyzer

Given the successful application of pXRF on the kimberlite whole rock powders, using a kimberlite-specific calibrated instrument in 'Mining Mode', the samples were subsequently re-analysed on a factory calibrated instrument in 'Mining Mode' (Figures 7, 8, 9) with He gas, and in 'Soil Mode' (Figures 10, 11). Of importance is the recognition that the factory-calibrated instrument may provide the correct value for any individual element (e.g. Figure 12). Alternately, the factory-calibrated instrument may not provide the correct value for any individual element (e.g. Figure 13). However, for statistical purposes, what is important is if the data for any element behaves in a regular fashion (e.g. Figure 13).

An analysis of variance was undertaken on both data sets. For 'Mining Mode', the best elements to discriminate the three kimberlite phases are Ti, Nb, Ba and the three poorest discriminators are Sr, Cr, Mg (Figure 14). For 'Soil Mode', the best elements to discriminate the three kimberlite phases are Ti, Cr, Zr and the three poorest discriminators are Th, Ca, Co (Figure 15). Note that the change in relative importance of Cr in the analysis of variance is that the data quality for Cr in 'Soil Mode' is better than the data from 'Mining Mode' with respect to degree of scatter and closeness of fit to the real (whole rock geochemistry) data. This is also observed in the data for Al, comparing the kimberlite-calibrated versus factory-calibrated instrument, with the latter exhibiting a significant degree of scatter as compared to the whole rock geochemical data.

Three highly discriminating elements from the analysis of variance for the 'Mining Mode' and 'Soil Mode' were chosen to undertake a Principal Component Analysis (PCA). There is a slight overlap between kimberlite phase U2VK and U3VK on the PC1 versus PC2 plot from the 'Mining Mode' data (Figure 16 Ti, Nb, with K instead of Zr). In contrast, there is good separation between all three kimberlite phases (U1VK, U2VK, and U3VK) on the PC1 versus PC2 plot from the 'Soil Mode' data (Figure 17; Ti, Cr, Zr).

Conclusions

The use of rock powders for analysis by pXRF provides acceptable results that can be utilized for statistical treatment to discriminate individual phases within the Whiskey kimberlite. The ability of the Niton XL3t GOLDD handheld XRF spectrometer to analyze for light elements (Si, Al, Mg) is seen as a significant advantage for classifying phases within the Whiskey kimberlite (i.e. Al, Mg; Kjarsgaard and Grunsky, 2008) and the Star kimberlite (i.e. Si, Mg, Al; Grunsky and Kjarsgaard, 2008). It is important to re-iterate that for any individual kimberlite body, the suite of elements that have high discriminating power can change, hence a handheld spectrometer that can analyze more of the diagnostic discriminating elements will ultimately be more useful. We further note that data acquired by pXRF spectrometry cannot eliminate the collection of high quality whole rock data and the two techniques should be used together

Data from a factory, non-specifically calibrated pXRF can provide meaningful data from rocks in both 'Mining Mode' or 'Soil Mode', or a combined element suite, from both analytical modes.

[1]Geological Survey of Canada, 601 Booth Street, Ottawa, Ontario K1A 0E8
[2]DeBeers Canada, 900-250 Ferrand Drive, Toronto, Ontario M3C 3G8

For more information, please contact E.C. Grunsky (Eric.Grunsky@NRCan-RNCan.gc.ca)

Natural Resources Canada | Ressources naturelles Canada

Publications in this series have not been edited; they are released as submitted by the author.

©Her Majesty the Queen in Right of Canada 2013

doi:10.4095/292446

This publication is available for free download through GEOSCAN (http://geoscan.ess.nrcan.gc.ca/).

Presented at the Society of Economic Geologists Minerals Colloquium, 2012 Prospectors and Developers Association Convention
Date presented: March 2012

Recommended citation
Grunsky, E.C., Kjarsgaard, B.A., Kurszlaukis, S., Seller, M., Knight, R., and Moroz, M., 2013. Classification of whole-rock geochemistry based on statistical treatment of whole-rock geochemical analyses and portable XRF analyses at the Attawapiskat kimberlite field of Ontario; Geological Survey of Canada, Scientific Presentation 15, poster. doi:10.4095/292446

2013

Canada